PAPER

Check for updates

Enhancing 3-acetyl-11-keto-β-boswellic acid skin permeation *via* nanostructured lipid carriers: integrating quality by design principles for risk estimation and optimization

Sakshi Priya, Vaibhavi Meghraj Desai, Hemraj Singh, Rajeev Taliyan and Gautam Singhvi ID *

3-Acetyl-11-keto-β-boswellic acid (AKBA), a bioactive compound derived from *Boswellia serrata*, exhibits significant anti-inflammatory and antioxidant properties, making it a promising candidate for treating inflammatory skin disorders. Its hydrophobic nature makes topical administration challenging. By developing nanostructured lipid carriers (NLCs), this work sought to enhance the skin penetration of AKBA. Quality-by-design principles were applied for the development of a robust formulation, where AKBA-NLCs were developed using a three-factor, three-level Box−Behnken design. AKBA-NLCs were prepared by the hot homogenization technique. The optimized formulation was further loaded into a gelling system, and its rheological parameters were evaluated. Further evaluation for *ex vivo* skin permeation and retention, along with other characteristics such as occlusivity, extrudability, and spreadability, was performed. Quality-by-design through *p*-value assessment highlighted that all three factors significantly affected particle size, and in the case of PDI, only lipid content showed a significant impact, whereas for entrapment efficiency, lipid and surfactant content were the governing factors. Based on the set constraints, the optimized batch of AKBA-NLCs exhibited a particle size of 173.700 ± 1.165 nm, a PDI of 0.323 ± 0.012, a zeta potential of −19.533 ± 0.493 mV, and an entrapment efficiency of 82.349 ± 3.223%. The *in vitro* release showed a prolonged release profile up to 56 h. When tested for cytotoxicity in the HaCaT cell line, the formulation was observed to be non-cytotoxic. The rheological data of the gel demonstrated a non-Newtonian, pseudo-plastic nature and indicated good structural strength. The *ex vivo* skin permeation of AKBA-NLCs was found to be 1.34 times higher than that *via* plain gel. Based on consistent results of viscosity, particle size integrity, and assay after one year of storage, the formulation was found to be stable. The formulation method used was simple and cost-effective, allowing for possible industrial scale-up. According to the findings, the NLC-loaded gel may prove to be a useful delivery strategy for the management of inflammatory skin conditions.

Introduction

3-Acetyl-11-keto-β-boswellic acid (AKBA) is a bioactive compound derived from the resin of *Boswellia serrata* (Salai/Salai guggul) from the family Burseraceae (Genus *Boswellia*), a plant renowned for its medicinal properties. Because of its various pharmacological effects, especially its strong anti-inflammatory and antioxidant properties, AKBA has become a noteworthy therapeutic agent. These characteristics make AKBA a viable option for treating various inflammatory conditions, including skin disorders such as acne, psoriasis, and atopic dermatitis, as well as chronic diseases such as rheumatoid arthritis and

neurodegenerative disorders. Studies have shown that AKBA selectively and non-competitively inhibits the enzyme 5-lipoxygenase, matrix metalloproteinases, and proinflammatory cytokines, which are essential for lowering inflammation linked to various inflammatory conditions.[1–7] The distinct physicochemical qualities of AKBA contribute to its therapeutic potential, but they also pose difficulties for efficient delivery. AKBA is a pentacyclic triterpene and has limited solubility under aqueous conditions. As AKBA is quickly eliminated from the body due to its hydrophobic nature (elimination half-life of 4.5 ± 0.55 h), its oral bioavailability is limited (<10%), resulting in suboptimal therapeutic levels in the bloodstream.[8] The compound's poor solubility causes insufficient absorption in the gastrointestinal tract, which reduces its potential for systemic treatments. This is just one of the major drawbacks of oral delivery.[2] In one study, to increase its oral bioavailability and *in vivo* anti-inflammatory

Industrial Research Laboratory, Department of Pharmacy, Birla Institute of Technology and Science, Pilani, Pilani Campus, Vidya Vihar, Pilani, Rajasthan 333031, India. E-mail: gautam.singhvi@pilani.bits-pilani.ac.in

action, AKBA was incorporated into a polylactic-*co*-glycolic acid-based nanoparticle formulation. According to a bioavailability study, AKBA-nanoparticles had a peak plasma concentration of AKBA that was almost six times greater. Additionally, when comparing AKBA-nanoparticles to free AKBA, $t_{1/2}$ and the total area under the curve were both increased by 2- and 9-fold, respectively.[9]

Topical administration methods that might maximize localized therapeutic effects while reducing systemic side effects are, therefore, becoming increasingly necessary. AKBA could be applied topically to the area of inflammation or skin conditions, optimizing its anti-inflammatory and antioxidant qualities.[2] However, topical delivery of AKBA is challenging due to high lipophilicity ($\log P$ 8), high molecular weight, poor solubility, and skin permeability.[7]

Novel and innovative delivery methods are necessary to overcome these delivery challenges. The permeation of the drug can be enhanced by making alterations in the properties of the drug or by using vehicles with high permeability potential. In order to increase the permeation of AKBA through topical delivery, recent research has investigated the use of nano-particles.[10] An AKBA-loaded polymeric nanomicelle gel was studied for topical delivery. The results exhibited enhanced anti-inflammatory action 24 h after delivery (81.1% compared to 44.1% for the AKBA gel) and after 13 days of activity (60.6% as opposed to 33.3% for the AKBA gel).[10] In another study, to enhance the topical administration, AKBA was developed as deformable nanospanlastics and elastic nanovesicles. With an enhancement ratio of 3.34, the proposed formulation demonstrated a significant increase in AKBA flux across the skin ($p < 0.05$) compared to AKBA dispersion.[11] Although polymeric nanomicelles and nanospanlastics exhibit potential for topical

administration of AKBA, their efficacy is restricted by several issues, such as being prone to aggregation or degeneration over time, which compromises their therapeutic efficacy and shelf life. Prior to the development of polymeric nanomicelles, there is a need for polymer synthesis, which makes the preparation process more complex and challenging for translation. Similarly, the scale-up potential of reported AKBA nano-formulations remains unexplored. To develop more dependable and efficient delivery systems for AKBA in topical applications, these constraints must be addressed.

Nanostructured lipid carriers (NLCs) present a promising delivery system for AKBA, effectively addressing many challenges associated with its topical application. Solid and liquid lipids utilized to prepare NLCs improve formulation stability and enable regulated release of the active component by increasing the solubility and bioavailability of poorly soluble compounds such as AKBA. This is particularly beneficial for AKBA, as it can penetrate deeper into the epidermis and dermis, crucial for treating inflammatory skin conditions such as psoriasis and atopic dermatitis. To ensure product quality and efficacy, risk estimation along with the Quality by Design (QbD) concept must be incorporated into the preparation of NLCs for the delivery of AKBA. The previously explored work on AKBA-loaded nanospanlastic formulation involved QbD-based screening and optimization. However, the formulation variables explored were limited, utilizing only a small number of experimental runs, which limits the ability to fully explore critical quality attributes and process interactions. Furthermore, there is limited discussion on formal risk assessment tools, such as Failure Mode and Effects Analysis (FMEA) and Relative Risk Matrix Analysis (RRMA), which are central to robust QbD implementation.
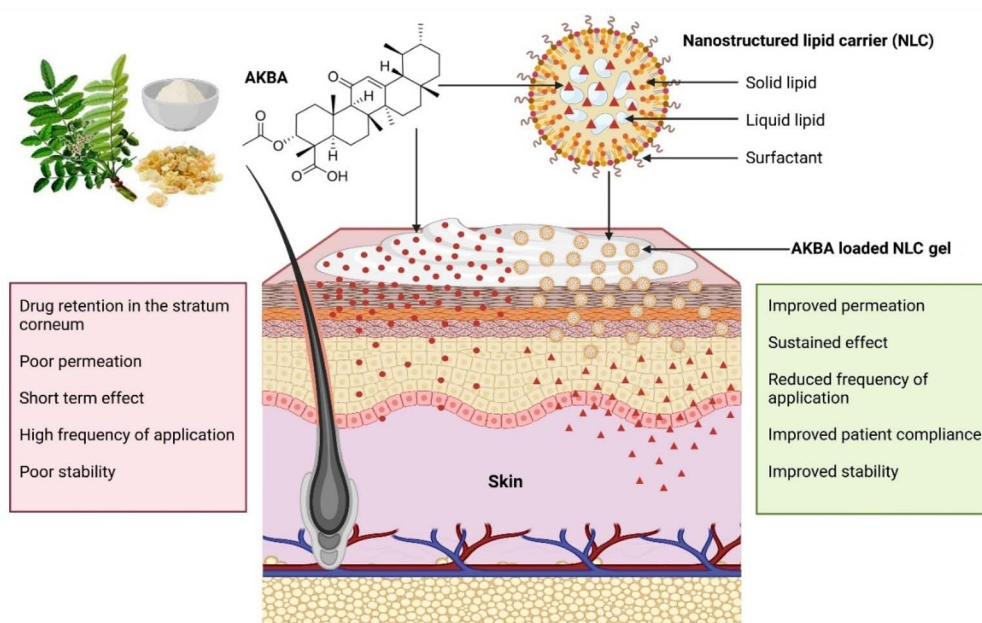

Fig. 1 Schematic representation of permeation of AKBA-NLCs across the skin barrier on topical administration and advantages. Created with https://Biorender.com.

Therefore, in this study, we aim to integrate QbD principles to optimize the formulation and manufacturing process of AKBA-loaded NLCs as a delivery strategy for enhanced skin permeation and retention. By employing a risk-based approach, we will identify and mitigate potential risks associated with the formulation and production of NLCs. The objectives of this research are to develop a robust and efficient method for the preparation of AKBA-loaded NLCs, to evaluate their skin permeation and retention properties, and to assess their therapeutic potential in treating skin disorders (Fig. 1). The results of this study will provide valuable insights into the development of novel and effective topical treatments for skin conditions, leveraging the synergistic benefits of AKBA loaded in NLCs.

Experimental section

Reagents and methods

AKBA was procured from Gurjar Phytochem Pvt. Ltd, Madhya Pradesh, India. Labrafac CC (caprylic/capric triglyceride) was obtained as gift samples from Gattefossé India. Dynasan 114 (trimyristin) was obtained as gift samples from Sasol Olefins & Surfactants (Germany), and Tween 80 was procured from S.D. Fine Chemicals (India). SEPINEO™ P 600 was used as a gelling agent, which was procured as a gift sample from SEPPIC. HPLC-grade methanol was purchased from Merck Pvt. Ltd (Mumbai, India). Milli-Q water was utilized throughout the study from a Milli-Q water purification system (Millipore, USA). All other solvents, reagents, and chemicals used were of analytical grade.

Incorporation of quality by design principles for formulation development

Incorporating systematic QbD principles in formulation development enhances pharmaceutical product quality. Throughout the product lifecycle, QbD is a methodical approach that places an emphasis on comprehending and managing the connections between critical quality attributes (CQAs) and critical process parameters (CPPs).[12,13] The variability that can affect the performance of NLC formulations can be identified and mitigated owing to this proactive approach. The creation of a quality target product profile (QTPP) at the beginning allows researchers to set precise goals that direct formulation development and guarantee that the finished product constantly satisfies safety and effectiveness requirements.[14] The importance of QbD resides in its capacity to improve the dependability of NLCs as a delivery method for AKBA, which will ultimately improve therapeutic results while lowering manufacturing risks. Integrating QbD principles also makes it easier to comply with regulations and to achieve continuous improvement, which is in line with industry standards established by agencies such as the FDA.[14]

Demarcating the quality target product profile and critical quality attributes

The QTPP is a comprehensive overview of the ideal product specifications to attain optimal safety and effectiveness. The QTPP, which included the different elements influencing the gel loaded with AKBA NLCs for topical distribution, was initially set up. CQAs were chosen to satisfy the QTPP, which controls the intended characteristics of the final product. The final product's CQAs ought to convey the quality necessary to satisfy the patient's requirements. Therefore, the QTPP and CQAs were chosen using literature and existing information prior to optimizing AKBA-loaded NLCs.[15]

Risk identification and assessment

To prevent any product failure, risk assessment studies were performed. The essential formulation and process variables for NLC formulation were screened using the Ishikawa diagram to have a better understanding of risks and to identify risk factors. Based on the possible difficulties influencing the formulation qualities, the risk-based matrix assessment was carried out. Using the risk estimation matrix, the critical material attributes (CMAs) and CPPs were chosen based on the low, medium, and high-level risk potential components.[15] In preliminary experimental trials, several variables were evaluated, including temperature, stirring speed, time, drug quantity, lipid amount, and surfactant amount. To perform FMEA, each of the chosen criteria was assessed for severity (S), probability (P), and occurrence (D). With a rank order of 1–5, the risk priority number (RPN) was determined. The CMAs and CPPs were screened and optimized using the derived RPN score.[14]

Systematic optimization of NLCs employing experimental design

Design of experiments (DoE) is a key component of QbD that permits the study of multiple variables at once and removes the restriction of a one-variable-at-a-time study design. In this study, a three-factor, three-level Box–Behnken design (BBD), which is a type of response surface methodology (RSM), was selected based on the parameters specified and the resources available.[16] Design Expert® (Version 13, Stat-Ease Inc., USA) software was used for the optimization.

Preparation of AKBA-loaded NLCs

Screening of various solid lipids, liquid lipids, and surfactants was already carried out for AKBA based on its solubility, particle size, and drug entrapment in our previous work. The desirable characteristics were shown by a combination of Dynasan 114, Labrafac CC, and Tween 80; hence, they were selected for further optimization.[17] As seen in Fig. 2, the NLCs were made using the probe sonication approach after hot emulsification. On a hot plate magnetic stirrer (Tarsons Spinot Digital, MC-02), the oil phase comprising 176 mg of Dynasan 144 and 75.4 mg of Labrafac CC was melted at about 70 ± 5 °C, and 10 mg of AKBA was dissolved in it. Then, 150 mg surfactant (Tween 80) solution in 10 mL of Milli Q water, which made up the aqueous phase, was heated to about 70 ± 5 °C. To create a pre-emulsion, the drug-containing lipid melt was then mixed with the preheated aqueous phase. The resulting pre-emulsion was stirred at 350 rpm for 15 min on a magnetic stirrer before being subjected to a probe sonication procedure with a Sonics Vibra-Cell VCX 750 watt ultrasonic sonicator for 5 min 30 s
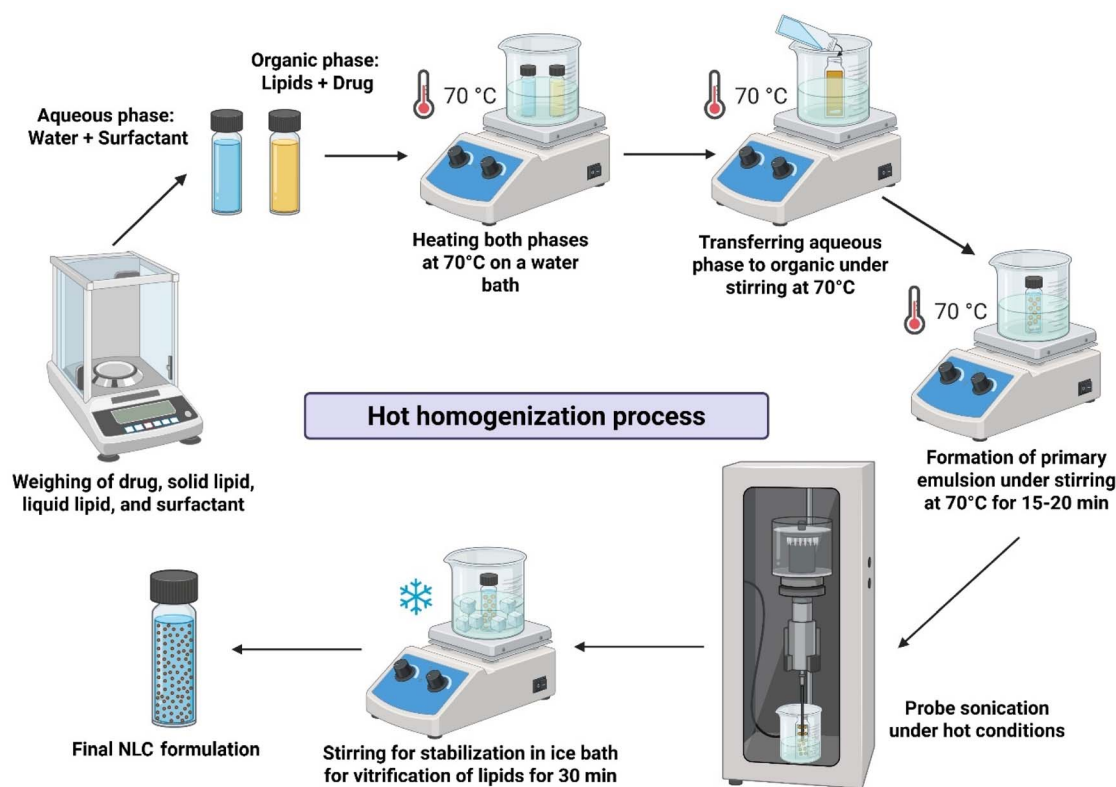
Fig. 2 Hot homogenization process for preparation of NLCs. Created with https://BioRender.com.

with 25% amplitude and 30 s pulses with 10 s intervals to reduce its size. The produced lipidic nanoparticles were vitrified by constantly stirring them in an ice bath.[18,19] The scale-up of the optimized batch was carried out up to 50 mL (5 times the optimum batch's volume). Within the design space, the sonication time, a process parameter, was changed. A probe sonicator, Sonics Vibra-Cell VCX 750 watt with a 3 mm tip diameter (capacity 1–10 mL) was used for the 10 mL batch, whereas a probe sonicator having a 13 mm diameter tip (capacity 10–250 mL) was used for the 50 mL batch size formulation. Evaluations were conducted on the impact of vessel diameter, dispersion volume, stirring duration, sonication time, and probe sonication capacity.[20]

Characterization of AKBA-loaded NLCs

Particle size, polydispersity index, & zeta potential. The distribution of particle size and zeta potential of the prepared AKBA-loaded NLCs was measured with the help of a Zetasizer (Malvern ZS nano 3600, UK) with a backscattering angle of 173° at a temperature of 25 ± 0.1 °C. Samples were diluted up to 15 times with Milli-Q water. Simultaneously, the hydrodynamic diameter distribution was also analysed in terms of polydispersity index (PDI). Similarly, to measure the zeta potential, the same instrument and similar procedure were adapted with cuvettes specially designed for this purpose. Every measurement was carried out in triplicate, requiring at least 50 runs for zeta potential analysis and 15 runs for particle size analysis.[15]

Entrapment efficiency and drug loading. AKBA NLC dispersion was centrifuged at 4000 rpm for 5 min and 4 °C using a REMI cooling centrifuge (CPR 24). A clear supernatant (200 µL) was collected, diluted with methanol, and centrifuged at 10 000 rpm for 30 min. The obtained supernatant (100 µL) was mixed with methanol and analyzed at 250 nm using an in-house developed and validated spectrophotometric method using a Jasco V-750 UV/Vis spectrophotometer (Tokyo, Japan).[12,17,21] The entrapment efficiency (EE) and drug loading were calculated using eqn (1) and (2).

$$\text{Entrapment efficiency} = \frac{\text{amount of drug entrapped}}{\text{total amount of drug present}} \times 100 \quad (1)$$

$$\text{Drug loading} = \frac{\text{weight of drug in NLCs}}{\text{weight of the formulation components and drug}} \times 100 \quad (2)$$

Morphological assessment of AKBA-loaded NLCs. Field emission scanning electron microscopy (FESEM) using an Apreo Switch XT microscope and transmission electron microscopy (TEM) with an FEI Tecnai – Netherlands; Model: G2 F30 S-Twin were used to characterize the morphology of the optimized NLC dispersion and analyze the surface topography of the optimized AKBA-loaded NLC formulation. The dispersion was applied and allowed to air dry on the coverslip for FESEM.

Samples were prepared on double-sided tape and gold-coated with a sputter coater unit (Quorum Q150 T ES, Quorum Technologies Ltd, UK) prior to morphological property evaluation. The images were taken between 1 and 10 kV with a magnification range of 10 000× to 75 000×. Uranium acetate staining was the first step in preparing the samples for TEM investigation, after which they were placed on a copper grid. Additionally, the dried sample was examined at 100 kV using TEM.[19]

Solid state characterization

Attenuated total reflection infrared spectroscopy (ATR-IR). The formulation's potential drug-excipient interactions were examined in freeze-dried samples. ATR spectroscopic equipment (Bruker, USA) was used to record the ATR-IR spectra of pure AKBA, the drug-free physical mixture, and the lyophilized AKBA-NLC formulation. A little portion of the sample was placed into the sample holder, and the IR spectra of the samples were recorded using the attenuated total reflection method. The infrared spectra were scanned at a resolution of 4 cm^{-1} in the 400–4000 cm^{-1} range.[10,11,22]

Differential scanning calorimetry (DSC). DSC analysis of the physical mixture of formulation composition, pure AKBA, and the lyophilized NLC sample was carried out using a Shimadzu DSC 60 Plus. The aluminium sample pan was filled with a 4 mg sample and sealed. The reference was an empty pan. The heating rate was maintained at 10 °C min^{-1}, while the gas flow rate was 30 mL min^{-1}. Between 30 and 400 °C, the analysis was conducted.[11]

Powder-X-ray diffraction (P-XRD). X-ray diffraction (XRD) analysis of pure AKBA, the physical mixture, and the lyophilized sample was carried out using P-XRD (Rigaku-Miniflex). Scanning angle was set at $3° \leq 2\theta \geq 40°$; scanning rate at 10° min^{-1} at a voltage of 40 kV using a beam current of 25 mA at 25 °C.[9]

***In vitro* drug release and kinetic modelling.** The dialysis membrane approach was used to study the *in vitro* release of AKBA-loaded NLCs. The media was a freshly made 70 : 30 ratio of pH 7.4 phosphate buffer saline to methanol with 40% polyethylene glycol 400 to maintain sink conditions.[10,23,24] A dialysis bag (Hi medium, MW: 12 to 14 kDa) was filled with roughly 2 mL of AKBA-loaded NLC formulation, which is equivalent to 2 mg of AKBA. After inserting the dialysis bag into the diffusion assembly, the entire setup was maintained at 37 °C in 20 mL of medium at 650 rpm on a magnetic stirrer. In order to maintain sink conditions, 1 mL aliquots were taken at intervals of 1, 2, 4, 6, 8, 12, 24, 30, 36, 48, and 56 hours and refilled with the same release media.[17] The experiment was run in triplicate, and the results were plotted using the *x*-axis for time and the *y*-axis for the percentage of cumulative drug release. Using the DDSolver Excel add-in, the findings were further examined for release pattern by kinetic modelling. To ascertain release kinetics, the release behavior was investigated for zero order, first order, Higuchi, Hixson–Crowell, and Korsmeyer–Peppas models.[14,25]

Cell viability assay. Cell viability was assessed through the 3-(4,5-dimethylthiazol-2-yl)-2,5-diphenyltetrazolium bromide (MTT) assay in HaCaT cell lines (procured from the National Centre for Cell Science, Pune) to evaluate the *in vitro* cytotoxicity of AKBA, blank NLCs, and AKBA-loaded NLCs. The cells were grown in 96-well plates in Dulbecco's modified Eagle's media supplemented with 10% Fetal bovine serum and 1% antibiotics at 37 °C under 5% CO$_2$ (4×10^3 cells per well). After 24 h incubation, the cells were treated with various concentrations of AKBA and AKBA-loaded NLC dispersion (0.64–10000 nM). After 48 h of treatment duration, 100 μL of MTT (1 mg mL^{-1}) was added to determine cytotoxicity. After 4 h incubation, formazan crystals were formed, which were dissolved in 100 μL of dimethylsulfoxide. Then, using a Synergy HT multi-detection microplate reader (Biotek, Winooski, VT), the absorbance was recorded at 570 and 630 nm.[26]

Preparation of the AKBA-loaded NLC nanogel. Optimized lipid nanocarriers were incorporated into the gel using SEPINEO™ P 600 (3.5%) as a gelling agent.[19] The nanocarrier formulation was slowly added to the gelling agent under stirring conditions and kept on stirring until a gel was formed. Similarly, a plain gel was prepared by adding water and an equivalent formulation quantity of the drug to the gelling agent. Then these gels were subjected to various characterization tests.

Characterization of the NLC-loaded nanogel

Physical examination, pH, assay, and particle size integrity of the NLC-loaded gel. The physical characteristics, such as lucidity, smoothness, and homogeneity, were assessed by visual observations. The pH of the gel was accessed using a digital pH meter (EcoTestr PH-1 pH Meter).[21] The quantity of medication was determined by dissolving 0.1 g of the gel in 1 mL of methanol for the test. The procedure was carried out in triplicate by collecting the gel from the tube's top, center, and bottom. The produced nanogel was redispersed in Milli-Q water and vortexed to create a transparent dispersion to determine the particle size integrity. As previously stated, a Malvern Zetasizer was used to measure the obtained dispersion for the particle size.[20]

Rheology. Viscosity, amplitude, and frequency sweep evaluations were performed on the NLC dispersion-loaded gel. The dispersion gel loaded with NLCs was measured using a Anton-Paar Pvt. Ltd rheometer MCR 92. A cone spindle with a 0.05 mm sample gap was employed. A constant shear rate of 50 s^{-1} was used for the frequency sweep, amplitude, and viscosity tests. The amplitude test was conducted at a constant angular frequency of 10 s^{-1} with shear strain ranging from 0.1 to 100%. The NLC-loaded gel formulation's viscoelastic behaviour and spreadability were assessed using the loss modulus (G'') and storage modulus (G').[20]

Spreadability. The ease with which a gel spreads when sheared is known as its spreadability. For this, 50 mg of the gel was weighed and placed between the two glass slides to assess spreadability. For 2 min, 50 g of weight was placed on top of each of the two slides to enable the gel to build a consistent layer between them. The weight was taken off after 2 min, and the diameter of the glass slide coated with gel was measured. The test was run in triplicate for both the prepared AKBA NLC gel and plain gel. The spreadability factor was computed using the formula in eqn (3), where A stands for the total sample

spread area (mm^2) and W for the total weight (g) applied to the sample.

$$\text{Spreadability factor} = \frac{A}{W} \qquad (3)$$

Spreadability is the region that the formulation covers on the skin once it is applied. A high degree of spreadability guarantees that there is enough dosage on the skin's surface to have a therapeutic effect.[20]

Extrudability. The amount of gel that emerges from the collapsible tube when a specific load is applied for a predetermined amount of time is known as extrudability. It is contingent upon the formulation's ultimate consistency. Patients are less likely to accept a product that is difficult to extrude. A 500 g weight was put close to the crimped end of an aluminium collapsible tube that had been filled with 20 g of nanogel and plain gel for the test. For the optimized gels, the extrudability was measured three times.[20]

Occlusivity. An *in vitro* occlusion test was used to examine the occlusive characteristics of both the plain gel and gel loaded with AKBA NLCs. For this, 10 mL of water was added to pre-weighed vials (15 mL capacity each) with an internal mouth diameter of 2 cm. Whatman filter paper (pore size 0.45 μ) was placed over the vials' mouths. On the filter paper, the AKBA-loaded NLC gel and plain gel were equally distributed. After that, the vials and a blank vial—that is, one without any sample applied—were kept at 32 ± 0.5 °C for 48 h. The vials were weighed both before and after 48 h to determine the amount of water lost. Eqn (4) was used to determine the occlusion factor.[20]

$$\text{Occlusion factor} =$$
$$\frac{(\text{water loss without sample}) - (\text{water loss with sample})}{(\text{water loss without sample})} \times 100 \qquad (4)$$

***Ex vivo* permeation evaluation and quantification of AKBA in skin layers.** For the skin permeation study, goat ear skin, which was prepared as described in the SI section, was used in *ex vivo* permeation assays to examine the impact of the NLC gel on the diffusion of AKBA through the skin. The Franz diffusion cell apparatus was used to mount the prepared skin. To maintain sink conditions, polyethylene glycol 400 was introduced to the receptor medium, which was filled with a 70 : 30 mix of pH 7.4 phosphate buffer saline and methanol. A 1.33 cm^2 surface area of the unjacketed vertical Franz diffusion cell was used to mount the treated skin. The skin was equilibrated for 1 h after the dermis side came into contact with the receptor media. Additionally, 350 mg of the prepared AKBA-loaded NLC gel was administered to the skin's surface, which was linked to the donor compartment. The assembly was set on a magnetic stirrer with a stirring speed of 120 rpm, and the temperature was kept at 32 ± 1 °C. To maintain sink conditions, a 1 mL aliquot was taken at various intervals for up to 24 h and replenished with the same release media.[15] The entire experiment was conducted in triplicate. From the *ex vivo* release data, the permeability

coefficient (K_p, cm h^{-1}) and steady-state transdermal flux (J_{ss}, mg h^{-1} cm^{-2}) were computed. Eqn (5) and (6) are used to determine the J_{ss} and K_p. The steady-state flux (J_{ss}), or dQ/dt, is indicated by the slope of the *ex vivo* diffusion study. The mass of the drug in the donor compartment (C_o) and J_{ss} were used to compute the permeability coefficient.[15]

$$J_{ss} = \frac{\mathrm{d}Q}{A\mathrm{d}t} \qquad (5)$$

$$K_p = \frac{J_{ss}}{C_o} \qquad (6)$$

The skin was taken out of the unjacketed vertical Franz diffusion cell assembly once the skin permeation investigation was finished. To get rid of extra gel, a tissue swab was used to wipe the skin's surface. For 6 h, the skin was left to dry. Methanol was added to the skin to extract AKBA after the viable portion was cut into pieces and placed into the vials. After being set aside for 6 h, the vials were sonicated for 1 h. To get rid of the debris, the collected aliquots were centrifuged for 20 min at 15 000 rpm. After that, 600 μL of the supernatant was extracted and passed through a 0.22 μm syringe filter. With additional dilution, the resultant sample was examined using the validated HPLC ($n = 3$) method.[15,27] Time on the x-axis and the percentage of AKBA that permeated with time on the y-axis were used to depict the permeation profile. The developed HPLC method was used to calculate the amount of AKBA retained in the skin.[27]

Data analysis and interpretation. ANOVA or Student's t-test, if suitable, or other statistical assessment criteria were used to statistically analyze all the data. Where appropriate, significance was assessed at a 95% confidence interval ($p < 0.05$).

Results and discussion

Outlining quality target product profiles and critical quality attributes

Beginning with the identification and specification of the QTPP, the NLC formulations were developed in accordance with the principles of QbD. Particle size, PDI, EE, stability, and percentage drug release are among the important CQAs that have been identified. These characteristics have a major impact on the product's quality and functionality. A thorough summary of the different QTPP elements and their corresponding CQAs for the NLC formulations is given in Tables 1 and 2. The tables also provide justifications for each chosen CQA, demonstrating the reasoning behind their selection.

Risk identification and assessment

The Ishikawa diagram, which was developed as an initial step to identify potential risks related to the formulation design, is depicted in Fig. 3. Finding the CMAs and CPPs that may affect the quality of the finished product is made easier with the help of this fishbone diagram. Tables 3 and 4, which describe risk estimation and factor screening using RRMA and FMEA, respectively, provide more information on risk analysis. Important parameters affecting the product's QTPP and CQAs

Table 1 Quality target product profile for AKBA-loaded NLCs

QTPP parameters	Target	Justification
Therapeutic indication	Anti-inflammatory	Anti-inflammatory agents are required to alleviate inflammation in cases of rheumatoid arthritis, psoriasis, osteoarthritis and other inflammatory conditions
Route of administration	Topical/local	This route is associated with enhanced patient compliance. Non-invasive and simple to use route
Site of activity	5-Lipoxygenase, IL-1 and TNF-α inhibition at the site of inflammation	By inhibiting the inflammatory modulators and arachidonic acid pathway at the site of inflammation, the symptoms can be alleviated
Dosage form	Topical gel	Being a gel, the dosage form can be easily applied as and when required, and the carrier system entrapped in the gel can act as a reservoir for sustained release of the active ingredient. Moreover, the oral administration is limited due to low solubility and the hepatic first-pass effect
Release pattern	Sustained release	To minimize the number of applications per day, a sustained release is required
Physical appearance	White gel with smooth texture	Smooth texture of the gel gives better spreadability and improves patient compliance
Particle size	<200 nm	Improves skin permeation
PDI	<0.3	Enhances formulation homogeneity and uniform drug delivery
EE	Maximum	Maximum entrapment ensures effective drug delivery at the site of application
Stability	No visible signs of instability at the time of preparation and throughout the product's shelf life	Any alterations in physical appearance may be a sign of drug degradation or interaction, which may produce harmful end products. Issues such as alteration in viscosity, pH, appearance, and crystal formation can impact the release and therapeutic potential

Table 2 Critical quality attributes for AKBA-loaded NLCs

QTPP elements	Justification
Particle size	For the drug to better penetrate the target site, particle size is essential. The surface area of smaller particles is greater, which can improve bioavailability and absorption. Furthermore, a smaller particle size aids in improved occlusion in topical formulations, ensuring that the drug remains in contact with the target area for an extended period of time, which is a crucial factor for localized therapies
PDI	The PDI indicates the uniformity of particle size distribution. A lower PDI ensures homogeneity, resulting in predictable and consistent drug release profiles, which is crucial for ensuring efficacy
EE	High EE maximizes drug loading, which is important for delivering therapeutic levels of the drug while minimizing the amount of formulation needed. This can also improve the overall efficiency of the drug delivery system and reduce dosing frequency
Stability	Stability is a critical attribute as it affects the shelf life, efficacy, and safety of the formulation. Instability can lead to drug degradation, altered release profiles, and loss of potency, all of which would negatively impact the product's quality and therapeutic effect. Ensuring stability is vital for maintaining the intended performance of the formulation over time
Drug release	Sustained drug release is essential in reducing the dosing frequency and retaining therapeutic levels of the drug over an extended period. For anti-inflammatory drugs, a sustained release helps provide a prolonged therapeutic effect, ensuring consistent reduction of inflammation and improving patient compliance by decreasing the need for frequent administration

were identified with the aid of preliminary experimental studies. The risk matrix showed that both particle size and EE were significantly impacted by the lipid concentration. The particle size and its distribution were largely determined by the concentrations of surfactants, whilst the particle size distribution was largely controlled by process variables including sonication time and stirring speed. Their RPN scores and an analysis of pertinent literature were used to guide the final selection of these parameters. Failure modes were ranked according to the extent of their possible effects using the RPN score. To differentiate between high-risk and low-risk

parameters, a cut-off value was applied to the RPN scores (Table 4). Critical factors were determined to be those with the highest RPN values (36 and 24). The amount of lipid, concentration of surfactant, temperature, rate of stirring, duration of probe sonication, vitrification, and stabilization were among these crucial elements.

Systematic optimization of NLCs employing experimental design

To statistically optimize the experimental variables, different batches of AKBA-loaded NLCs were developed using the Box–
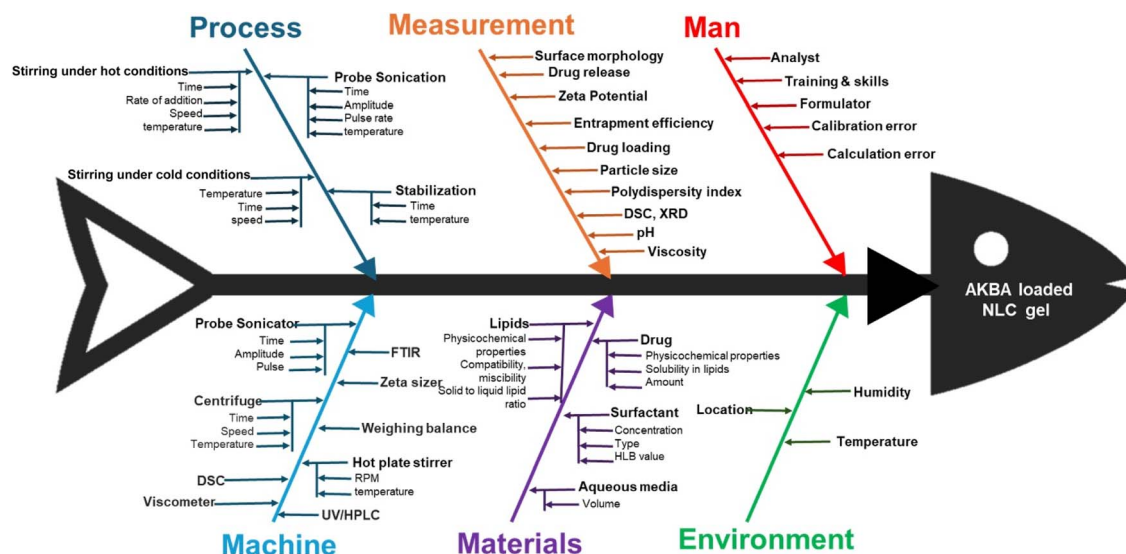
Fig. 3   Risk identification using the Ishikawa diagram.

Table 3   Risk estimation matrix

CQAs	Material Attributes			Process Parameters		
	Drug	Lipids	Surfactant (Type and concentration)	Stirring speed, time, and temperature	Probe sonication time	Vitrification temperature and time
Particle size	Low	High	High	High	High	High
PDI	Low	High	High	High	High	High
EE	High	High	High	Low	High	High
Zeta Potential	Low	High	Medium	Low	Medium	Medium

Behnken Design (BBD). One of its strongest rationales is its efficiency in requiring fewer experimental runs than a full factorial design and central composite design while still effectively modelling both main effects and interactions among three or more independent variables across three levels. This allows for comprehensive optimization with reduced cost, time, and resource investment while maintaining the quality of the data. BBD is rotatable or nearly rotatable, providing uniform precision for estimation of model coefficients. Additionally, BBD models quadratic response surfaces, making it suitable for detecting curvatures and optimizing complex responses relevant to formulation performance and quality.[28,29]

The design's numerical independent variables, the amount of lipid (A), the amount of surfactant (B), and the sonication time (C), were adjusted at three different levels while holding all other variables constant over numerous tests. The preliminary trials were used to determine the higher and lower values of the independent variables, as indicated in Table 5. The mean particle size (Y_1), PDI (Y_2), and EE (Y_3) were used to measure the dependent variables or responses. The 17 BBD runs with 5 centre points were used to examine the main effect, interaction effect, and quadratic effect (Table 6). Following the characterization, the response values were entered into various models, such as first order, second order, quadratic models, etc., using Design Expert® (Version 13, Stat Ease Inc.).
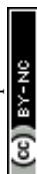
Table 4   Screening of factors based on FME analysis

Property	Material attributes	Failure mode	Effect on CQA	P	S	D	RPN
AKBA-physical	Moisture content	High	The high moisture content will cause degradation, leading to the introduction of impurities as well as microbial contamination, affecting safety	1	4	1	4
	Purity	Low	Low purity will lead to impurities, causing toxicity and affecting safety	1	4	1	4
AKBA-chemical	Stability	Low	Poor stability of AKBA will cause structural changes, leading to impurities, causing toxicity, and affecting safety	1	4	1	4
Excipients							
Lipids	Grade	Change in grade	A change in grade can affect drug-excipient compatibility, affecting efficacy	1	3	1	3
	Purity	Low	Low purity will lead to impurities, causing toxicity and affecting safety	1	4	1	4
	Polymorphic form	Change in form	Structural changes in the excipient due to a shift in polymorphic forms can affect drug-excipient compatibility, drug leaching, affecting efficacy	1	3	3	9
Surfactant	Concentration	High	High surfactant can cause excess size reduction, affecting entrapment, causing drug leaching, and further reducing efficacy	1	3	2	6

Process	Process parameters	Failure mode	Effect on CQA	P	S	D	RPN
Mixing and stirring	Time	Less than optimum	Non-uniform mixing can cause phase separation, further reducing entrapment and efficacy	2	3	4	24
	Rate of addition	Fast	A faster rate of addition can cause phase separation, further reducing entrapment and efficacy	3	3	4	36
	Temperature	Lower than 70 °C	Improper vitrification can cause drug leaching, further reducing entrapment and efficacy	2	3	4	24
	RPM value	Low	Non-uniform mixing can cause phase separation, further reducing entrapment and efficacy	2	3	4	24
Probe sonication	Time	Less	A change in time can lead to improper particle size reduction, affecting efficacy	1	3	2	6
	Amplitude	Low	A change in amplitude can lead to improper particle size reduction, affecting efficacy	1	3	2	6
	Pulse	Alteration	If the pulse program is altered, it can cause overheating of the probe, leading to formulation instability and affecting efficacy	1	3	2	6
	Temperature	Lower than 70 °C	A reduction in temperature during probe sonication can solidify lipid nanoparticles inappropriately, causing drug leaching, reduced entrapment, and affecting efficacy	3	3	4	36
Vitrification	Temperature	High	Improper temperature during vitrification can solidify lipid nanoparticles inappropriately, causing drug leaching, reduced entrapment, and affecting efficacy	3	3	4	36
	Speed	Low	If the stirring speed is improper, it can affect the stabilization of nanoparticles, further affecting efficacy	2	3	4	24

Table 4 (*Contd.*)

Process	Process parameters	Failure mode	Effect on CQA	P	S	D	RPN
	Time	Less	Insufficient time during vitrification can solidify lipid nanoparticles inappropriately, causing drug leaching, reduced entrapment, and affecting efficacy	2	3	4	24
Stabilization	Time	Less	Insufficient time during stabilization can cause drug leaching, reduced entrapment, and affect efficacy	2	3	4	24
	Temperature	High	Stabilization under higher temperatures can reduce stability, causing drug leaching, reduced entrapment, and affecting efficacy	2	3	4	24

Table 5 Selection of independent variables and responses for Box–Behnken design

		Coded level and actual values		
Independent variables		High	Medium	Low
A	Lipid content	300 mg	200 mg	100 mg
B	Surfactant content	150 mg	100 mg	50 mg
C	Sonication time	6 min	4 min	2 min
Dependent variables				Goals
Y_1	Particle size			In range
Y_2	PDI			Minimize
Y_3	EE			Maximize

Analysis of the dependent variable for prepared NLCs

Impact of formulation variables on particle size. For the particle size, both linear and quadratic models were considered based on key statistical parameters, including predicted R^2, adjusted R^2, p-value, and PRESS. Although the linear model had a lower PRESS value and a positive predicted R^2, the quadratic model was chosen. This is because it is the highest-order polynomial in which the additional terms are statistically significant, the model is not aliased, and it provides the highest R^2 value. The average particle size across the 17 experimental runs of NLCs ranged from 150.6 nm to 320.4 nm, as shown in Table 6.

The quadratic model, along with the ANOVA results for the particle size, revealed that factor A (lipid content), factor B (surfactant concentration), factor C (sonication time), and the

Table 6 Box–Behnken design with observed responses for trials

		Factor			Response		
Std	Run	A: lipid content (mg)	B: surfactant (mg)	C: sonication time (min)	Y_1: particle size (nm)	Y_2: PDI	Y_3: EE (%)
1	2	100	50	4	208.45	0.408	30.726
2	4	300	50	4	272.1	0.347	65
3	17	100	150	4	166.15	0.442	68.965
4	8	300	150	4	205.3	0.326	83.28
5	5	100	100	2	216.3	0.414	52.634
6	1	300	100	2	250.6	0.394	55.995
7	13	100	100	6	159.3	0.438	48.401
8	6	300	100	6	180	0.299	62.648
9	3	200	50	2	320.4	0.37	47.258
10	9	200	150	2	279.5	0.451	82.204
11	7	200	50	6	175.9	0.249	44.032
12	16	200	150	6	162.1	0.378	89.059
13	15	200	100	4	150.6	0.326	63.253
14	11	200	100	4	169.6	0.334	58.884
15	10	200	100	4	177.2	0.246	61.302
16	12	200	100	4	159.8	0.288	75.954
17	14	200	100	4	171.1	0.257	64.554

higher-order terms of factors B and C were statistically significant. Insignificant terms were removed, resulting in a reduced quadratic model in eqn (7) with an F-value of 20.35. The Lack of Fit (LOF) F-value of 4.56 indicated that the LOF was not significant compared to the pure error. LOF represents the deviation from the best-fit model and serves as a measure to evaluate how well the model fits the experimental data. An insignificant LOF suggests that the model is appropriate for fitting the experimental results.

$$Y_1 = 168.69 + 19.73A - 20.47B - 48.69C + 40.51B^2 + 29.06C^2 \quad (7)$$

A positive sign in the regression equations indicates a synergistic effect, which means that a rise in the relevant input variable will result in a rise in the response value. In contrast, a negative sign denotes an antagonistic impact, meaning that a higher level of the input variable would result in a lower response value. Increasing lipid content generally leads to larger particle sizes because more lipid provides more constituents for droplet and particle formation, promoting aggregation and growth. Conversely, a higher surfactant concentration exhibits a negative effect on particle size because surfactants lower the interfacial tension, stabilize droplets during emulsification, and prevent coalescence, thus yielding finer particles. Increasing sonication time generally leads to a reduction in the particle size. This is because extended sonication applies greater shear forces and energy input, which efficiently break down larger lipid droplets into smaller particles, resulting in a finer dispersion.[30]

In regression eqn (4), surfactant content shows a negative effect on particle size. The influence of surfactant amount and its interactions on particle size can be visualized using the 3D response surface plots in Fig. 4. In the figure, the effect of varying lipid content, surfactant concentration, and sonication time on particle size is depicted. At higher levels of lipid and surfactant, the particle size is moderate (Fig. 4A). This is because, while an increase in lipid content tends to increase the particle size, a higher surfactant concentration counteracts this by reducing the size, resulting in an intermediate particle size. For lipid content and sonication time (Fig. 4B), the particle size is also moderate when both factors are at high levels. As lipid content increases, particle size grows, but extended sonication

time reduces it, leading to a balanced outcome. In the case of surfactant concentration and sonication time (Fig. 4C), the particle size is minimized when both factors are at high levels, as increasing both results in a reduction of particle size.

Impact of formulation variables on PDI. Table 6 displays the average values for the PDI throughout all 17 experimental runs of AKBA-NLCs, which varied from 0.246 to 0.451. Both linear and quadratic models were taken into consideration for PDI based on important statistical measures, such as PRESS, p-value, adjusted R^2, and predicted R^2. Because it represents the highest-order polynomial where additional terms are statistically significant, is not aliased, and yielded the highest R^2 value, the quadratic model was selected even though the linear model had a lower PRESS value and a positive predicted R^2. A reduced quadratic model was developed after the selection of the quadratic model. The ANOVA findings indicated that component A (lipid content) and its higher-order term (A^2) were significant, while other inconsequential terms were eliminated. The statistical significance of the model is indicated by its F-value of 4.74. Furthermore, the model is appropriate for fitting the experimental data, as indicated by the LOF F-value of 2.44, which implies that the LOF is insignificant in comparison to the pure error. The reduced model for PDI, represented in terms of the coded values of the chosen independent components, is given by the following regression equation (eqn (8)):

$$Y_2 = 0.3221 - 0.0420A + 0.0614A^2 \quad (8)$$

Lipid content was the sole significant factor for PDI; no interaction effects between other components were observed. The one-factor effects graph (Fig. 5A), which shows the linear impact of altering the level of a single factor, makes this clear. Predicting the results at the factor's low (-1) and high ($+1$) values produces the graph. Since lipid content is the sole significant component impacting PDI, it is the only one plotted in this instance. The graph demonstrates a curvature effect, with PDI decreasing as lipid content increases from a low to a high level.

Impact of formulation variables on entrapment efficiency. As shown in Table 6, the average EE values for the 17 experimental runs of AKBA-NLCs varied from 30.726% to 89.059%. A linear
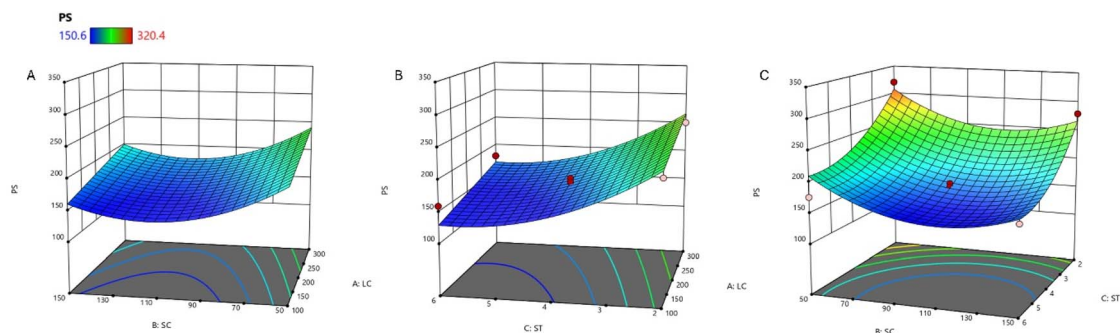

Fig. 4 Three-dimensional response surface plots showing the interaction effect of varying (A) lipid content with surfactant concentration; (B) lipid content with sonication time; and (C) surfactant concentration with sonication time on particle size.
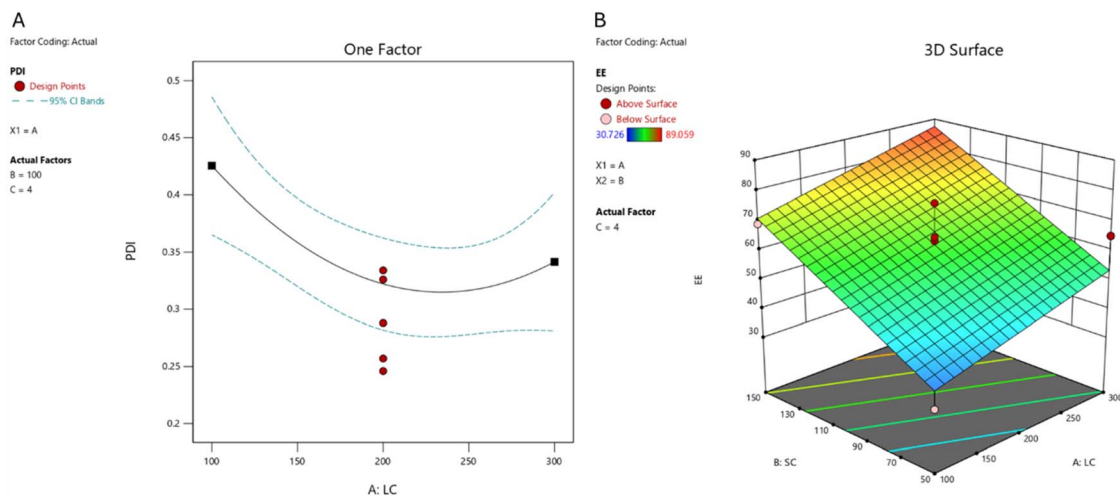
Fig. 5 (A) One-factor plot to study the effect of lipid content on PDI; (B) three-dimensional surface plot for entrapment efficiency to study the interaction effect of lipid content and surfactant content.

model was suggested based on important statistical variables, such as PRESS, p-value, adjusted R^2, and predicted R^2. The best option for this data set was the linear model, which showed a lower PRESS value and a positive predicted R^2.

A simplified linear model with a model F-value of 24.72 was obtained by removing other inconsequential components from the linear model and ANOVA findings, which showed that factors A (lipid content) and B (surfactant concentration) were significant. The model fits the experimental data well, as indicated by the LOF F-value of 1.47, which indicates that the LOF is negligible in comparison to the pure error. Below is the regression equation (eqn (9)) for EE, which is given in terms of the coded values of the independent factors that were chosen.

$$Y_3 = 62.01 + 8.27A + 17.06B \tag{9}$$

The impact of different lipid and surfactant concentrations on EE is depicted in Fig. 5B. Higher levels are shown in red areas, and lower levels are shown in blue areas. The plot demonstrates that EE is high when both lipid and surfactant concentrations are high. This is because a higher lipid content makes more of the drug soluble, and the outer layer of surfactants aids in the solubilization of an additional fraction.[31] The surface map lacks curvature because the data fit a linear model.

Optimization of NLCs

Table 7 provides specific limitations for each element and response to optimize the NLC formulation. The objective was to identify the ideal values for the independent variables to produce NLCs with the largest % EE, the minimum PDI, and the required particle size. A solution table was created using Design-Expert software, and the composition with the highest desirability score (0.768) was chosen for validation. The optimized batch, which was prepared in triplicate, produced an EE of 82.349 ± 3.223%, a PDI of 0.323 ± 0.012, and a particle size of 173.700 ± 1.165 nm, all of which were within the design space (Fig. 6). As recommended by the software, the optimized batch's

composition consisted of 251.434 mg of lipid, 150 mg of surfactant, and a sonication time of 5.30 min. For scaling up and additional characterisation, this optimized batch was selected. The optimized formulation's responses were noted, and the software's projected values were contrasted with the values seen in the experiment to confirm the validity of the constructed mathematical model. According to Table 7, the percentage deviation fell within the permissible limit.

Application of ANOVA

ANOVA, F tests, and correlation coefficients were used to statistically evaluate the impact of the input components on the dependent response variables at a 95% significance level (P 0.05) (Table 8). The ANOVA results for the responses Y_1-particle size, Y_2-PDI, and Y_3-EE (%) are displayed in Table 8. An ANOVA examination of the model's adequacy and the three selected input elements revealed that there were sufficient signals to route the design space and predict the selected response variables.

Table 7 Constraints set for formulation optimization

Name	Goal	Lower limit	Upper limit
A: lipid concentration (mg)	In range	100	300
B: surfactant concentration (mg)	In range	50	150
C: sonication time (min)	In range	2	6
Particle size (nm)	In range	150.6	200
PDI	Minimize	0.246	0.451
EE (%)	Maximize	30.726	89.059

Deviation (%) calculation of NLC formulation

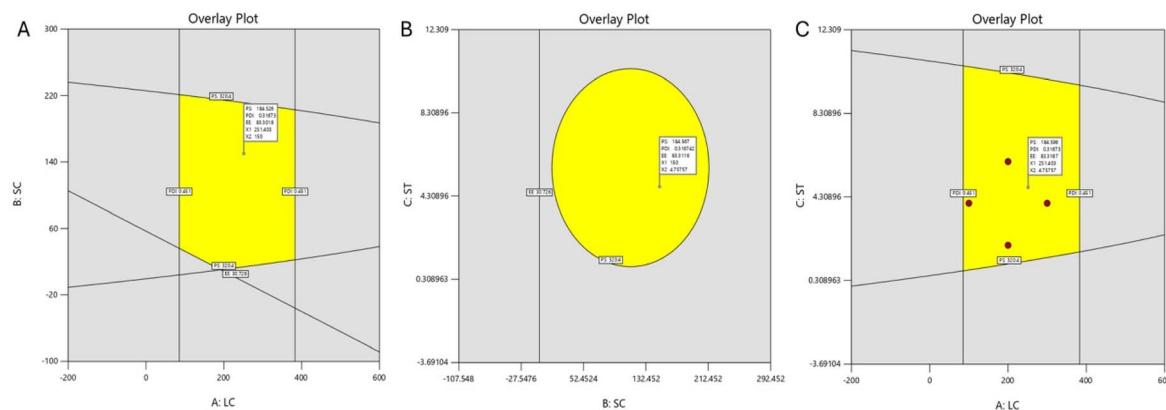| Response	Predicted	Actual	Deviation
Particle size (nm)	179.489	173.700	5.789
PDI	0.317	0.323	0.006
EE (%)	83.326	82.349	0.977

Fig. 6 Design space for (A) lipid content and surfactant content; (B) surfactant content and sonication time; (C) lipid content and sonication time.

Table 8 Particle size, polydispersity index, and entrapment efficiency ANOVA response

Response	Particle size		PDI		EE	
Source	F-Value	p-Value	F-Value	p-Value	F-Value	p-Value
Model (significant)	20.35	<0.0001	4.74	0.0268	24.72	<0.0001
A: lipid concentration	8.67	0.0133	4.45	0.0535	9.41	0.0083
B: surfactant concentration	9.34	0.0109	—	—	40.02	<0.0001
C: sonication time	52.83	<0.0001	—	—	—	—
A^2	—	—	5.03	0.0416	—	—
B^2	19.31	0.0011	—	—	—	—
C^2	9.94	0.0092	—	—	—	—

Exploration of scale-up potential

To examine the reproducibility at a higher volume, the optimized batch was further scaled up five times. It was discovered that the scale-up formulation's properties were the same as those of the batch that was optimized. The 5-fold scaled-up batch was assessed for EE (86.431 ± 2.811%), particle size (171.233 ± 3.955 nm) and PDI (0.353 ± 0.036). The formulation was stable, as indicated by its zeta potential of −20 ± 0.7 mV. A change in formulation parameters, such as the NLC's size, PDI, and EE, could result from increasing the batch size. Scaling up nanoparticles significantly changes mass transfer and momentum. However, even in scaled-up batches, the formulation features remained unchanged by the reduced formulation processing stages and the lack of organic solvents in this preparation technique. This suggested that the product could be appropriate for industrial translation.[18]

Characterization of AKBA-loaded NLCs

Particle size, PDI, & zeta potential. Values of all the AKBA-loaded NLC batches for particle size and PDI ranged between 150.6 and 200 nm and 0.246 and 0.451, respectively. The optimized batch had a particle size of 173.700 ± 1.165 nm, a PDI of 0.323 ± 0.012, and a zeta potential of −19.533 ± 0.493 mV (Fig. 7). The negative zeta potential is due to the carboxylic and hydroxylic groups in the lipids used. These values depicted a narrow particle size distribution profile & led

to the development of homogeneous nanoparticles. Nanoparticles with a size less than 200 nm are considered suitable for topical applications as they can improve skin permeation, facilitating enhanced drug delivery to the target site. Furthermore, the PDI of the optimized batch indicates a relatively narrow particle size distribution. The zeta potential indicates good stability of the NLC dispersion, as a value above ±10 mV generally indicates sufficient electrostatic repulsion to prevent particle aggregation, thereby ensuring the long-term stability of the formulation.[32]

Entrapment efficiency and drug loading. All batches had EE percentages ranging from 30.726 to 89.059%. The optimized batch had a drug loading of 2.010 ± 0.077% and an EE of 82.349 ± 3.223%. Achieving such a high EE rating was made possible by the concentration of surfactants and the lipid content.

Morphological assessment of AKBA-loaded NLCs. Using TEM and FESEM, the optimized AKBA NLC dispersion was morphologically characterized. Particle sizes ranged from 89 nm to 260 nm, according to the FESEM image (Fig. 8A and B). The microscopic pictures showed that the particles had a smooth surface and were homogeneous. The TEM images revealed that the nanoparticles, regardless of the different lipid matrices used, exhibited a spherical morphology with well-defined surfaces. Moreover, the encapsulation of AKBA did not compromise the structural integrity of the nanoparticles (Fig. 8C and D).
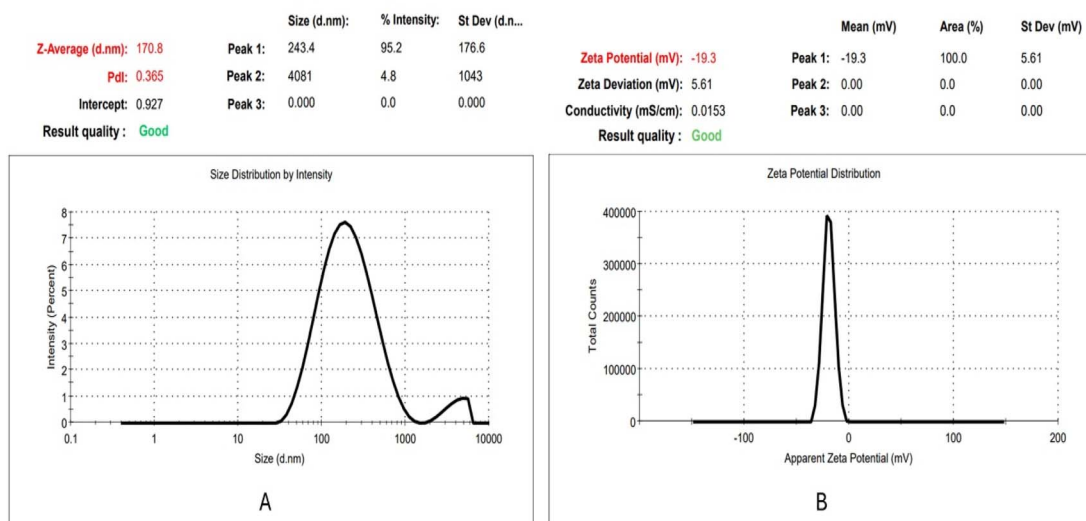
Fig. 7 (A) Particle size and PDI of optimized formulation; (B) zeta potential of optimized formulation.
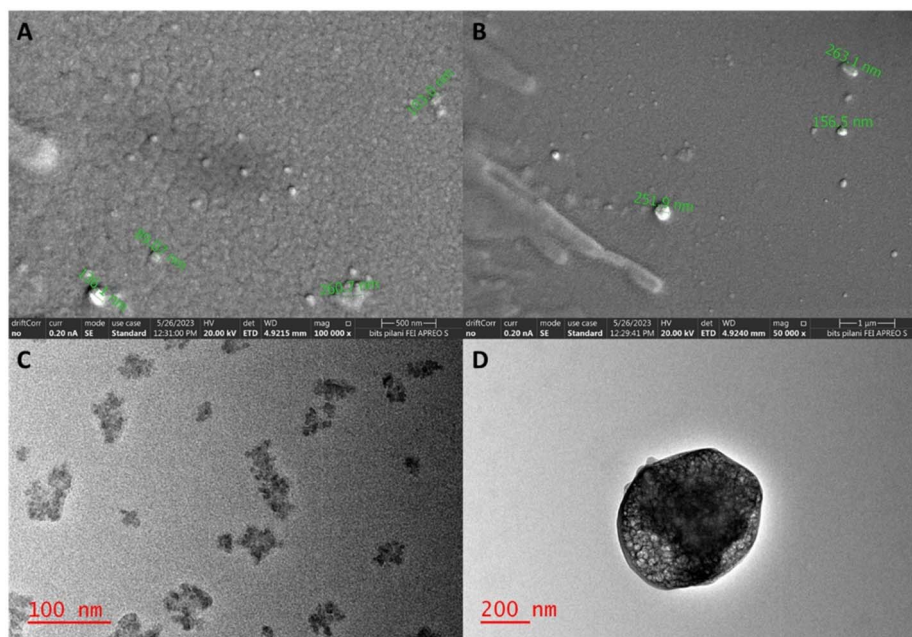

Fig. 8 Morphological assessment of AKBA NLC dispersion using (A and B) SEM; (C and D) TEM.

Solid state characterization

Attenuated total reflection infrared spectroscopy (ATR-IR). There were notable peaks at 1262, 1728, 2909, and 2312 cm^{-1} in the drug ATR-IR spectra (% transmittance *vs.* wavenumber) of AKBA (Fig. 9). The existence of carboxylic acid (C=O stretching vibration) was confirmed by the strong band seen in the drug at 1728 cm^{-1}. The C–H stretching vibration was identified as the cause of the distinctive peak at 2909 cm^{-1}.[22]

Upon incorporation into the optimized NLC formulation, the ATR-IR spectra preserved the characteristic peaks of AKBA and the excipient matrix, with minor shifts and decreased intensity observed in the principal peaks. These spectral changes are

indicative of weak physical interactions such as hydrogen bonding, van der Waals forces, or dipole–dipole interactions between AKBA and the lipid/surfactant environment. The absence of new peaks and the conservation of core vibrational bands of AKBA confirm that encapsulation occurs without significant alteration of the chemical structure of the drug, supporting the physical stability of the formulation. These findings are in line with those of a previously reported study that showed no interactions between the drug and other components of the AKBA-loaded nanospanlastic formulations in the ATR-IR spectrum, which displayed the characteristic peaks of the drug and excipients with a minor shift. Therefore, the developed NLC formulation preserves the identity of AKBA
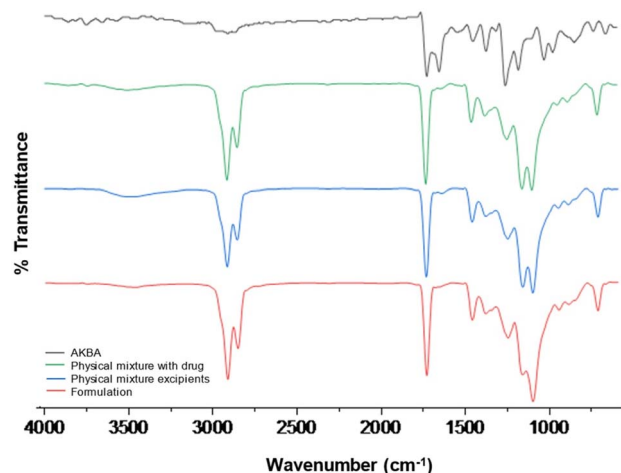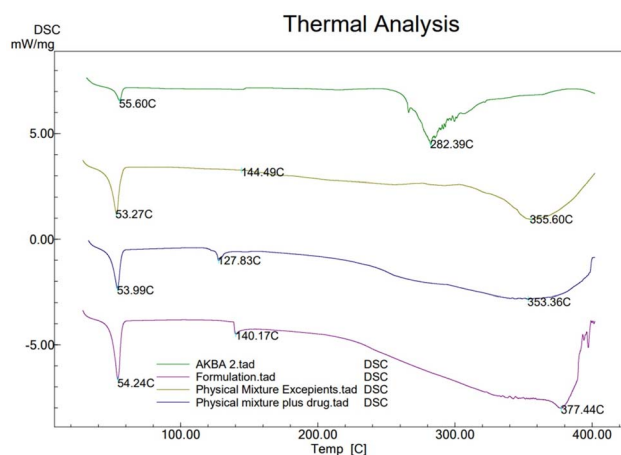
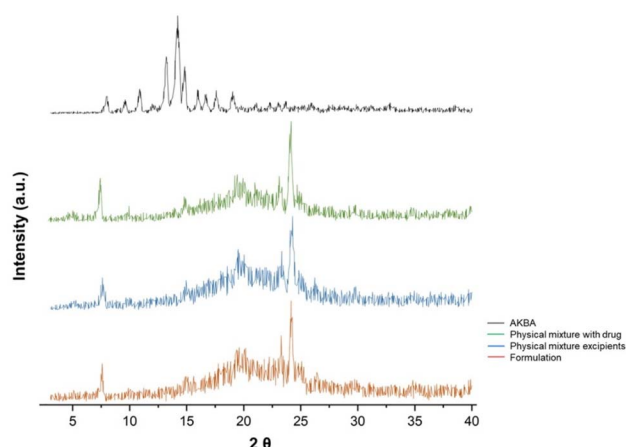**Fig. 9** ATR-IR spectra of AKBA, physical mixture with drug, physical mixture of excipients, and formulation.

Fig. 11 X-ray diffractograms of AKBA, physical mixture with drug, physical mixture of excipients, and formulation.

while stabilizing intermolecular interactions crucial for formulation performance.[11]

Differential scanning calorimetry (DSC). DSC aids in the analysis of the physical state, thermal behavior, and impact of interactions between drugs and excipients. The crystallinity of AKBA was demonstrated by the endothermic melting peak at 282.39 °C shown in the DSC thermogram of AKBA (Fig. 10).[11] A new endothermic peak that may represent the formulation's ingredients appeared in the physical combination containing only excipients at 355.6 °C. Due to AKBA's entrapment in the NLCs and its amorphous dispersion, which raised the phase transition temperature of the NLC dispersion, the improved formula revealed a shift in the endothermic peak to 377.44 °C and the removal of the AKBA peak. These findings are in line with those found in the case of nanospanlastic formulation that displayed a complete disappearance of the endothermic peak of AKBA in the DSC thermogram due to the loading of AKBA within the vesicles in the amorphous form.[11]

Powder-X-ray diffraction (P-XRD). The results of ATR-IR and DSC are in close agreement with those of XRD. For pure drug, sharp and well-defined peaks were observed (Fig. 11). In the case of formulation, a broad pattern was observed, suggesting an amorphous nature of AKBA in encapsulated NLCs. The presence of a few sharp peaks indicates crystallinity of lipids.[11]

***In vitro* drug release and kinetic modelling.** The % cumulative drug release for the free drug reached 96.18 ± 5.26% in 8 h, whereas the NLC formulation took 56 h to reach 95.99 ± 6.50% drug release. Fig. 12 depicts the cumulative *in vitro* drug release of AKBA from NLCs. The results indicated that the drug was released in 56 h from NLCs, suggesting controlled or sustained release over a period. Whereas, in the case of a free drug, in 8 h, a significant amount of drug was released, indicating a faster release rate than the NLC formulation. This suggests that the free drug may not possess sustained release characteristics and require frequent dosing to maintain therapeutic levels.[11]
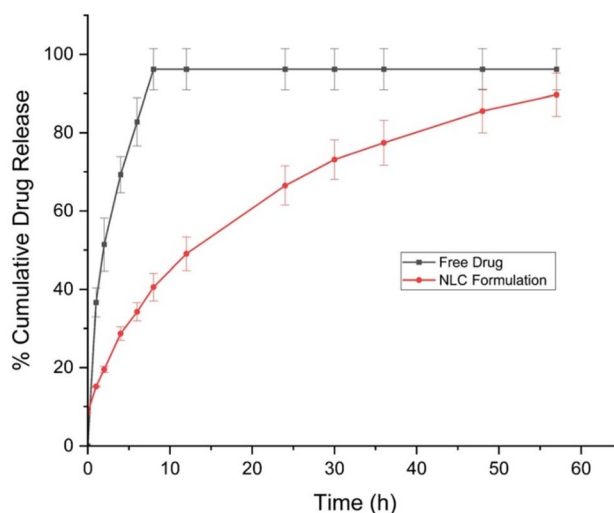

Fig. 10 DSC thermograms of AKBA, physical mixture with drug, physical mixture of excipients, and formulation.

Fig. 12 *In vitro* release study for free drug and NLC formulation.

Table 9 *In vitro* release kinetics modelling as calculated by the DDSolver Excel plug-In for the optimized NLC batch

Model name	AKBA loaded NLCs			Free AKBA		
	R^2	AIC	MSC	R^2	AIC	MSC
Zero-order model	0.7753	97.418	1.125	−1.4034	124.047	−1.805
First order model	0.9921	57.178	4.479	0.9822	65.201	3.098
Higuchi model	0.9901	59.959	4.247	0.1357	111.774	−0.782
Korsmeyer–Peppas model	0.9896	61.441	4.123	0.8738	89.540	1.070
Hixon–Crowell model	0.9723	72.286	3.220	0.2249	110.467	−0.673
T_{50} (h)	13.098			2.035		
T_{80} (h)	30.413			4.725		
MDT (h)	17.080			2.654		
F_1 (%) AKBA NLCs *vs.* AKBA	37.057					
F_2 (%) AKBA NLCs *vs.* AKBA	23.164					

The selection of a suitable release model plays an important role in defining the release profile of any drug delivery system. Linear regression analysis was performed for the zero order model ($M_t/M_0 = K_0 \times t$), first order model ($\ln(M_0 - M_t) = K_1 \times t$), Higuchi model ($M_t/M_0 = K_H \times t^{1/2}$), Korsmeyer–Peppas model ($M_t/M_0 = K_{KP} \times t^n$), and Hixon–Crowell model ($M_0^{1/3} - M_t^{1/3} = K_{HC} \times t$) where K is the kinetic constant and M_t/M_0 is the fraction of NLCs released at time t. Zero-order kinetics represents a constant drug release from the system irrespective of the drug concentration, whereas in the case of first-order release kinetics, the release of the drug is directly proportional to its concentration. In the case of certain controlled-release drug delivery systems, when the drug release is dependent on both diffusion through the matrix and dissolution in the solvent, it shows the best fit to the Higuchi model of release. When the drug shows diffusion-controlled release, to understand the type of diffusion, it is necessary to check the n value of the data obtained by fitting the data into the Korsmeyer–Peppas model of release. This n value represents the type of diffusion occurring, and in the case of drug delivery systems where the surface of drug release is constantly changing, the Hixon–Crowell model shows the best fit. The best model was chosen based on the highest R^2 value, Model Selection Criterion (MSC) value, and the lowest Akaike Information Criterion (AIC) value.

The mathematical model was adjusted accordingly, and the results were obtained, which are represented in Table 9. It is clearly visible that the release profile of the formulation shows the best fit into the first-order model due to the observed linearity in its graph. Thus, the release profile shows direct proportionality to the concentration gradient and is a function of the amount of drug remaining in the formulation.

Cell viability assay. The cells of the epidermal layer of skin are 95% keratinocytes, and the HaCaT cell line, being an immortalized human keratinocyte, is most suitable to check the safety of the drug and formulation *via* a cell viability study. As shown in Fig. 13, AKBA was observed to be reasonably non-toxic against HaCaT cells. The cell viability of more than 90%, for free AKBA, black NLC dispersion, as well as AKBA-NLC dispersion, was noted even up to a high dose of 10 μM concentration. From the obtained data, it can be deduced that the formulation excipients are also not cytotoxic towards the keratinocyte cells.[26]
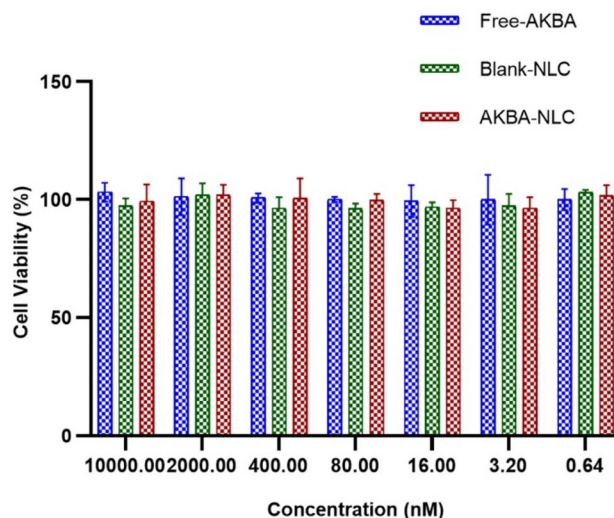
Fig. 13 Representation of *in vitro* cell viability study of free AKBA, blank NLC dispersion, and AKBA-loaded NLCs performed in the HaCaT cell line.

Characterization of the NLC-loaded nanogel

Physical examination, pH, assay, and particle size integrity of the nanocarrier-loaded gel. The prepared AKBA-NLC-loaded gel had good homogeneity and was white in color with a pH of 5.5. The drug content in the gel was found to be 82.943 ± 8.606%, and the particle size of NLCs loaded in the gel was 213.033 ± 8.727 nm. The stability of the gel was analysed by assessing the assay and particle integrity after one year. The assay was found to be 102.635 ± 9.915% and the particle size was 229.925 ± 12.735 nm. The consistency in these values demonstrated that the gel had good stability at 2–8 °C.

Rheology. A cone type Anton Paar Rheometer (CP25) with a gap of 0.05 mm was used to assess the viscosity, amplitude sweep test, and frequency sweep test of the plain gel and the NLC-loaded gel. The cone-shaped geometry allowed for a decreased gap height on the sample with continuous shear.

Viscosity. From the graphs shown in Fig. 14, viscosity *vs.* shear rate, it was observed that the viscosity of the plain gel and NLC-loaded gel decreases with increasing shear rate. The flow
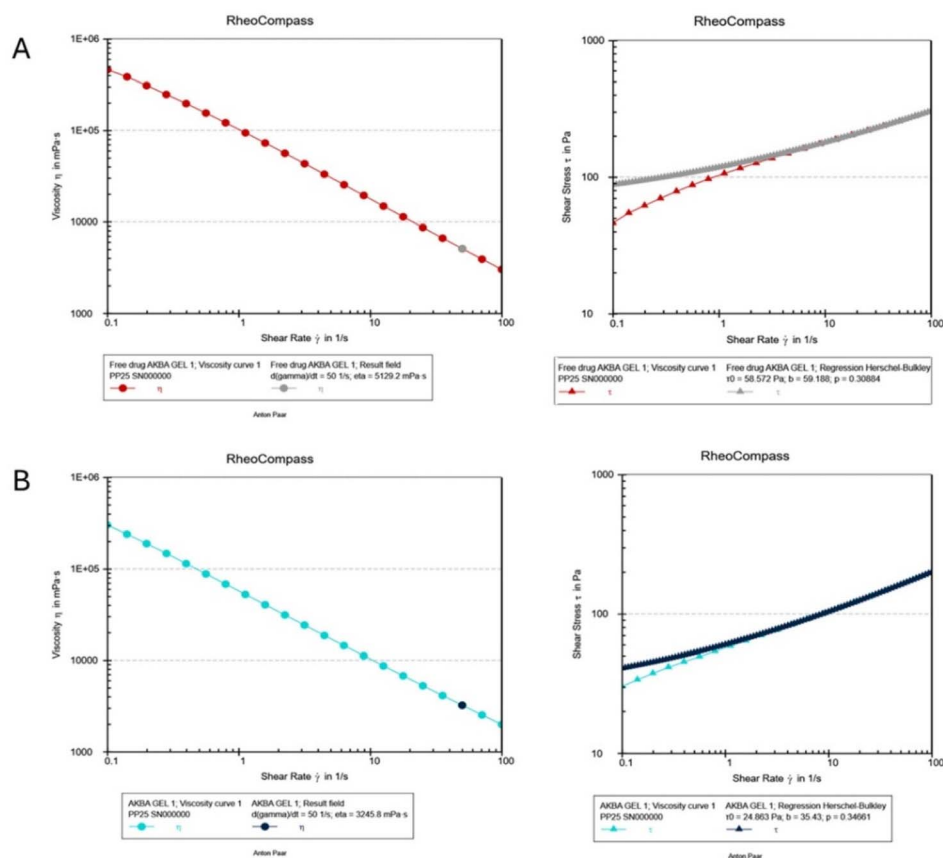
Fig. 14 Viscosity of (A) the plain gel and (B) NLC-loaded gel.

behaviour index value (p value) is also less than 1, which indicates the non-Newtonian and pseudo-plastic nature of the gel. A reduction in viscosity with increased shear rate was observed, a property crucial for topical systems as it ensures ease of application and spreading upon gentle application, yet allows the gel to regain its structure post-application for improved retention on the skin.[33] The viscosity of the plain gel (5129 mPa s) was higher than that of the NLC-loaded gel (3245.8 mPa s). The torque value (τ_0), which is the value of shear stress when the shear rate is zero, is higher in the case of plain gel (58.572 Pa) than in the NLC-loaded gel (24.863 Pa), suggesting a better spreading and extruding potential of the NLC-loaded gel. The b value, which is a constant related to the consistency of the fluid, is also higher for the plain gel (59.188) than that for the NLC-loaded gel (35.43). This makes the NLC-loaded gel more patient-compliant and easy for topical application.[19] The stability of the gel was checked after 1 year, and the viscosity was found to be consistent (3684.4 mPa s), suggesting that the formulation is stable at room temperature.

Amplitude sweep. An amplitude sweep test involves the application of a small oscillatory strain or deformation to a material at differing amplitudes while keeping the frequency constant. The resulting stress response is then measured to determine the material's viscoelastic properties, such as the linear viscoelastic region, yield stress, and strain-hardening behaviour. The amplitude of deformation is increased from

a small value until the material begins to exhibit nonlinear behaviour. Fig. S1 presents storage modulus G' (units – Pa; elastic portion) and loss modulus G'' (units – Pa; viscous portion) vs. shear strain (%). The values of $G' > G''$ in the plain gel and NLC-loaded gel confirm the gel-like viscoelastic solid behaviour due to the linkage formation. This governance of G' signifies a strong internal network proficient in preserving shape and withstanding flow under low stress, imparting the necessary structural integrity to the formulation. This profile also indicates that the formulation is stable against minor physical and mechanical stresses encountered during application, thus ensuring formulation reliability.[19]

Frequency sweep. A frequency sweep test involves application of a small oscillatory strain or deformation to a material at differing frequencies by keeping the strain amplitude constant. The resulting stress response is then analysed to determine the material's viscoelastic properties, such as its storage and loss moduli, viscous and elastic components, and relaxation behaviour. The frequency of deformation is changed over a range of values from low to high. Fig. S2 presents the frequency sweep test graph, i.e., G' and G'' (Pa; y-axis) vs. angular frequency (units – rad s^{-1}; x-axis). The structural behavior of the developed gels is better understood owing to this graph. The high degree of crosslinking in this is confirmed by $G' > G''$, indicating the developed gel's good structural strength.[19]
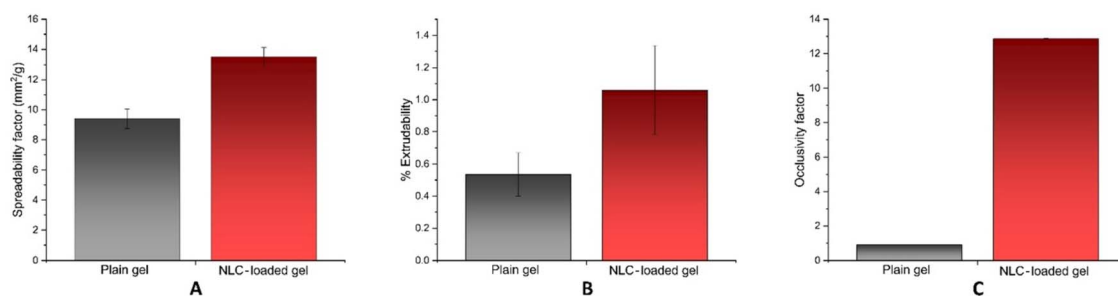
Fig. 15   (A) Spreadability study; (B) extrudability study; (C) occlusivity study of the plain gel and NLC-loaded gel.

Spreadability. The spreadability factor of the NLC-loaded gel (13.516 ± 0.612 mm^2 g^{-1}) was found to be 1.4 times higher than that of the plain gel (9.392 ± 0.646 mm^2 g^{-1}). The optimized formulation showed good spreadability, which will ensure proper distribution of the gel on the skin surface, greater contact surface, and improved absorption, as shown in Fig. 15.

Extrudability. The extrudability of the NLC-loaded gel ($1.058 \pm 0.277\%$) was found to be 1.97 times higher than that of the plain gel ($0.535 \pm 0.134\%$), as shown in Fig. 15. The optimized formulation showed good extrudability, which will ensure better patient compliance.

Occlusivity. The formulation's capacity to create an occlusive layer on the skin's surface was used to calculate the percentage of water loss from the skin. Since there were no lipids in the formulation, the simple gel had the lowest occlusion factor ($0.903 \pm 0.015\%$) and the most water loss from evaporation.[34] After 48 h, the occlusion factor for both the plain gel and NLCs loaded with AKBA was assessed. The findings showed that the occlusive properties of the NLC-loaded gel ($12.866 \pm 0.019\%$) were 14 times greater than those of the simple gel. Fig. 15 displays the obtained occlusion factor. The occlusion analysis showed that because of the larger surface area of the nanoparticles, the AKBA formulation based on NLCs had a higher occlusion factor than the ordinary gel of AKBA. According to this study, the formulation of NLCs has a high occlusive character and lowers the trans-epidermal water loss (TEWL). Because less TEWL hydrates the skin, less water loss enhances penetration.

***Ex vivo* permeation evaluation and quantification of the AKBA NLC gel in skin.** The amount of AKBA penetration through goat ear skin was measured using the established method. In 24 h, the total amount of medication that penetrated the epidermal tissue through the AKBA-loaded NLC gel was 60.944 ± 2.635 µg cm^{-2}, 1.34 times more than that through the ordinary gel (45.367 ± 0.139 µg cm^{-2}). Fig. 16 displays the *ex vivo* skin penetration profile of AKBA from NLCs. The transdermal flow of the free drug gel was 2.211 µg cm^{-2} h^{-1}, 1.36 times lower than that of the NLC gel, which had a transdermal flux of 3.012 µg cm^{-2} h^{-1}. The free drug-loaded gel's permeability coefficient was 0.006 cm h^{-1}, while that of the NLC formulation was 0.008 cm h^{-1}. It was discovered that the enhanced penetration of the NLC formulation was caused by the nano-size of dispersion and the development of an occlusive
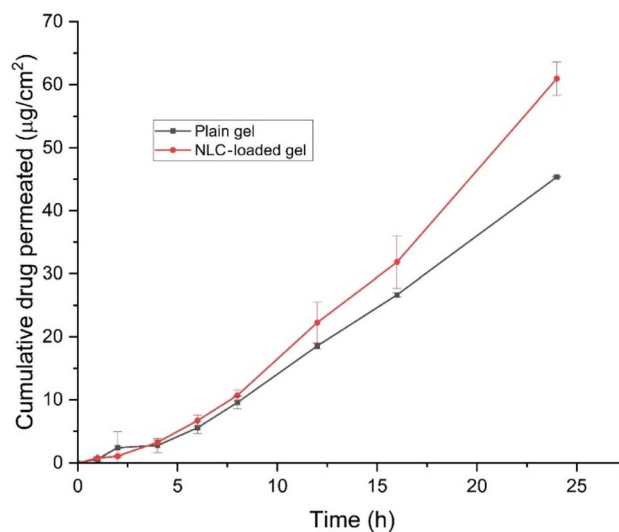

Fig. 16   *Ex vivo* skin permeation study for the plain gel and NLC-loaded gel.

film on the skin. Hydration increases skin lipid swelling and enhances skin penetration. The NLC-loaded gel and plain gel were observed to retain 12.682 ± 2.373 µg cm^{-2} and 24.549 ± 1.729 µg cm^{-2} of the drug in the skin, respectively. The study showed that the gel loaded with NLCs had better skin penetration.

The NLC matrix developed by incorporating solid (Dynasan 114) and liquid (Labrafac CC) lipids is less ordered and more fluid, which allows a higher drug solubilization and sustained release, while the nanoscale size of NLCs ensures intimate and prolonged contact with the stratum corneum, enabling close intercalation with the dermal lipids. Interaction of Dynasan 114 with skin occurs due to susceptibility towards lipase-mediated degradation once it penetrates, and its crystalline structure may influence skin diffusion and drug release kinetics.[35] Labrafac CC also helps in alteration of skin barrier properties by affecting the intercellular lipid matrix of stratum corneum, causing disruption of packed lipid regions and improving drug diffusion. The surfactant Tween 80, along with increasing solubility of the active agent, also enhances skin permeability by increasing drug partitioning into the skin. When combined with other enhancers, it can disturb the arrangement of

orthorhombic and lamellar lipid domains critical for skin barrier integrity, leading to enhanced permeability and diffusivity of drugs through the skin.[36]

NLCs, when applied topically, form a thin, occlusive layer over the skin, considerably reducing TEWL and increasing local hydration. This temporary swelling of the stratum corneum generates microenvironments that further improve drug diffusion into deeper layers. In addition to these intercellular effects, NLCs utilize the transappendageal route, efficiently accessing and accruing in hair follicles and glandular structures, which function as reservoirs for deeper diffusion and prolonged drug release. The combined action of small particle size, the occlusion-induced hydration effect, solid–liquid lipid matrix design, surfactant action, and appendageal targeting enables NLCs to elevate skin permeation and retention of AKBA compared to conventional formulations.[15]

Conclusion

In this work, the principles of QbD were applied for systematic formulation optimization through risk estimation. A three-factor, three-level BBD design was applied to establish the effect of chosen independent variables—lipid concentration, surfactant amount, and time of sonication—on the selected response variables: particle size, PDI, and % EE. The NLC-loaded gel was prepared with a simple process, which was economic and did not utilize any sophisticated techniques or instruments. It was discovered that the optimized NLC formulation had a higher % EE, uniform dispersion, and a smaller (nanorange) particle size. The *in vitro* results showed a sustained release and *ex vivo* permeation of the NLC-loaded gel showed 1.34-fold higher permeation when compared with the plain gel. Based on the viscosity, assay, and particle size integrity, the formulation was found to be stable. The developed gel was safe for topical use and did not exhibit any signs of irritation or inflammation, suggesting skin compatibility (Fig. S3).

According to the study outcomes, AKBA loaded into NLCs could be considered a promising lipid-based nanocarrier technology that can improve the drug's topical penetration and absorption. Enough contact time is provided by the enhanced skin penetration over an extended period to effectively manage inflammatory skin conditions. Additionally, this formulation's potential for industrial scale-up is supported by the simple and affordable preparation method used. Future research can further refine these formulations for large-scale manufacture and assess their pharmacological qualities through *in vivo* experiments.

Ethical statement

All animal procedures (skin irritation test) were performed as per the guidelines of 'Committee for the Purpose of Control and Supervision of Experiments on Animals (CPCSEA)', India, with the animal protocol (IAEC/RES/34/07) for Care and Use of Laboratory Animals approved by the Institutional Animal Ethics Committee (IAEC) of Birla Institute of Technology and Science, Pilani University.

Author contributions

Sakshi Priya: writing – original draft, validation, methodology, investigation, data curation. Vaibhavi Meghraj Desai: writing – original draft, methodology, formal analysis, data curation. Hemraj Singh: methodology, data curation. Rajeev Taliyan: supervision, project administration. Gautam Singhvi: writing – review & editing, resources, conceptualization, supervision, project administration.

Conflicts of interest

The authors declare no competing interests.

Data availability

The data supporting this article have been included as part of the supplementary information (SI). Supplementary information: graphical data for amplitude and frequency sweep test and *in vivo* skin irritation study for the developed AKBA NLCs gel. See DOI: https://doi.org/10.1039/d5na00445d.

Acknowledgements

References

1 S. Priya and G. Singhvi, Insights into the anti-inflammatory and anti-arthritic potential of 3-Acetyl-11-keto-β-Boswellic Acid as a therapeutic approach in Rheumatoid Arthritis, *Expert Opin. Invest. Drugs*, 2023, **32**(10), 867–871, DOI: 10.1080/13543784.2023.2269838.

2 T. Yang, X. Lin, H. Li, X. Zhou, F. Fan, J. Yang, *et al.*, Acetyl-11-Keto-Beta Boswellic Acid (AKBA) Protects Lens Epithelial Cells Against H2O2-Induced Oxidative Injury and Attenuates Cataract Progression by Activating Keap1/Nrf2/HO-1 Signaling, *Front. Pharmacol*, 2022, **13**(July), 1–14, DOI: 10.3389/fphar.2022.927871.

3 S. Singh, A. Khajuria, S. C. Taneja, R. K. Johri, J. Singh and G. N. Qazi, Boswellic acids: A leukotriene inhibitor also effective through topical application in inflammatory disorders, *Phytomedicine*, 2008, **15**(6–7), 400–407, DOI: 10.1016/j.phymed.2007.11.019.

4 D. Taherzadeh, V. Baradaran Rahimi, H. Amiri, S. Ehtiati, R. Yahyazadeh, S. I. Hashemy, *et al.*, Acetyl-11-Keto-β-Boswellic Acid (AKBA) Prevents Lipopolysaccharide-Induced Inflammation and Cytotoxicity on H9C2 Cells, *Evid. base Compl. Alternative Med.*, 2022, **2022**, 1–10, DOI: 10.1155/2022/2620710.

5 Y. S. Park, J. H. Lee, J. A. Harwalkar, J. Bondar, H. Safayhi and M. Golubic, Acetyl-11-Keto-ß-Boswellic Acid (Akba) is

Cytotoxic for Meningioma Cells and Inhibits Phosphorylation of the Extracellular-Signal Regulated Kinase 1 and 2, *Adv. Exp. Med. Biol.*, 2002, **507**, 387–393, DOI: **10.1007/978-1-4615-0193-0_60**.

6 Y. Ding, Y. Qiao, M. Wang, H. Zhang, L. Li, Y. Zhang, *et al.*, Enhanced Neuroprotection of Acetyl-11-Keto-β-Boswellic Acid (AKBA)-Loaded O-Carboxymethyl Chitosan Nanoparticles Through Antioxidant and Anti-Inflammatory Pathways, *Mol. Neurobiol.*, 2016, **53**(6), 3842–3853, DOI: **10.1007/s12035-015-9333-9**.

7 A. F. Raja, F. Ali, I. A. Khan, A. S. Shawl and D. S. Arora, Acetyl-11-keto-β-boswellic acid (AKBA); Targeting oral cavity pathogens, *BMC Res. Notes*, 2011, **4**(406), 1–8, DOI: **10.1186/1756-0500-4-406**.

8 Y. Gong, X. Jiang, S. Yang, Y. Huang, J. Hong, Y. Ma, *et al.*, The Biological Activity of 3-O-Acetyl-11-keto-β-Boswellic Acid in Nervous System Diseases, *NeuroMol. Med.*, 2022, **24**(4), 374–384, DOI: **10.1007/s12017-022-08707-0**.

9 K. Bairwa and S. M. Jachak, Development and optimisation of 3-Acetyl-11-keto-β-boswellic acid loaded poly-lactic-co-glycolic acid-nanoparticles with enhanced oral bioavailability and in-vivo anti-inflammatory activity in rats, *J. Pharm. Pharmacol.*, 2015, **67**(9), 1188–1197, DOI: **10.1111/jphp.12420**.

10 A. Goel, F. J. Ahmad, R. M. Singh and G. N. Singh, 3-Acetyl-11-keto-β-boswellic acid loaded-polymeric nanomicelles for topical anti-inflammatory and anti-arthritic activity, *J. Pharm. Pharmacol.*, 2010, **62**(2), 273–278, DOI: **10.1211/jpp.62.02.0016**.

11 F. Badria and E. Mazyed, Formulation of nanospanlastics as a promising approach for improving the topical delivery of a natural leukotriene inhibitor (3-acetyl-11-keto-β-boswellic acid): Statistical optimization, in vitro characterization, and ex vivo permeation study, *Drug Des., Dev. Ther.*, 2020, **14**, 3697–3721, DOI: **10.2147/DDDT.S265167**.

12 T. Waghule, V. K. Rapalli, G. Singhvi, P. Manchanda, N. Hans, S. K. Dubey, *et al.*, Voriconazole loaded nanostructured lipid carriers based topical delivery system: QbD based designing, characterization, in-vitro and ex-vivo evaluation, *J. Drug Delivery Sci. Technol.*, 2019, **52**(April), 303–315, DOI: **10.1016/j.jddst.2019.04.026**.

13 A. Zafar, O. A. Alsaidan, M. S. Mohamed, M. Yasir and M. Khalid, Development of Gentamicin Bilosomes Laden In Situ Gel for Topical Ocular Delivery: Optimization, In Vitro Characterization, Toxicity, and Anti-microbial Evaluation, *Adv. Pharm. Bull.*, 2024, **14**(3), 646–664, DOI: **10.34172/apb.2024.057**.

14 S. Priya, G. Srividya, N. S. Chandra, P. P. Singh, R. N. Saha, P. Sathe, *et al.*, Loteprednol etabonate loaded lyotropic liquid crystalline nanoparticles in-situ ophthalmic gel: Qbd driven optimization and in-vitro, ex-vivo evidence of sustained precorneal residence time, *J. Drug Delivery Sci. Technol.*, 2023, **89**(October), 105081, DOI: **10.1016/j.jddst.2023.105081**.

15 V. K. Rapalli, S. Sharma, A. Roy and G. Singhvi, Design and dermatokinetic evaluation of Apremilast loaded nanostructured lipid carriers embedded gel for topical delivery: A potential approach for improved permeation and prolong skin deposition, *Colloids Surf., B*, 2021, **206**(June), 111945, DOI: **10.1016/j.colsurfb.2021.111945**.

16 Y. Tomar, S. Maheshwari, S. Gorantla and G. Singhvi, Curcumin loaded liquid crystalline nanoparticles for enhanced topical application : Design , characterization , ex vivo and dermatokinetic evaluation, *J. Drug Delivery Sci. Technol.*, 2024, **92**(January), 105391, DOI: **10.1016/j.jddst.2024.105391**.

17 S. Priya, V. M. Desai and G. Singhvi, Spectroscopic method to estimate 3-Acetyl-11-keto-β-boswellic acid in complex lipid nanocarriers and skin matrices, *Results Chem.*, 2024, **7**, 101261, DOI: **10.1016/j.rechem.2023.101261**.

18 V. K. Rapalli, V. Kaul, T. Waghule, S. Gorantla, S. Sharma, A. Roy, *et al.*, Curcumin loaded nanostructured lipid carriers for enhanced skin retained topical delivery: optimization, scale-up, in-vitro characterization and assessment of ex-vivo skin deposition, *Eur. J. Pharm. Sci.*, 2020, **152**(April), 105438, DOI: **10.1016/j.ejps.2020.105438**.

19 S. Gorantla, E. R. Puppala, V. G. M. Naidu, R. N. Saha and G. Singhvi, Hyaluronic acid-coated proglycosomes for topical delivery of tofacitinib in rheumatoid arthritis condition: Formulation design, in vitro, ex vivo characterization, and in vivo efficacy studies, *Int. J. Biol. Macromol.*, 2023, **224**(June 2022), 207–222, DOI: **10.1016/j.ijbiomac.2022.10.117**.

20 A. Mahmood, V. K. Rapalli, S. Gorantla, T. Waghule and G. Singhvi, Dermatokinetic assessment of luliconazole-loaded nanostructured lipid carriers (NLCs) for topical delivery: QbD-driven design, optimization, and in vitro and ex vivo evaluations, *Drug Delivery Transl. Res.*, 2022, **12**(5), 1118–1135, DOI: **10.1007/S13346-021-00986-7**.

21 T. Waghule, V. K. Rapalli, G. Singhvi, S. Gorantla, A. Khosa, S. K. Dubey, *et al.*, Design of temozolomide-loaded proliposomes and lipid crystal nanoparticles with industrial feasible approaches: comparative assessment of drug loading, entrapment efficiency, and stability at plasma pH, *J. Liposome Res.*, 2021, **31**(2), 158–168, DOI: **10.1080/08982104.2020.1748648**.

22 A. Khan, A. Al-Harrasi, N. U. Rehman, R. Sarwar, T. Ahmad, R. Ghaffar, *et al.*, Loading AKBA on surface of silver nanoparticles to improve their sedative-hypnotic and anti-inflammatory efficacies, *Nanomedicine*, 2019, **14**(21), 2783–2798, DOI: **10.2217/nnm-2019-0211**.

23 A. Zafar, M. Yasir, L. Singh, M. Jafar, M. H. Warsi and D. S. Panda, Luteolin-loaded Invasomes Gel for Transdermal Delivery: Development, Optimization, in-vitro, and Preclinical Evaluation, *J. Oleo Sci.*, 2024, **73**(9), 1221–1240, DOI: **10.5650/jos.ess24041**.

24 I. A. Tekko, M. C. Bonner, R. D. Bowen and A. C. Williams, Permeation of bioactive constituents from Arnica montana preparations through human skin in-vitro, *J. Pharm. Pharmacol.*, 2006, **58**(9), 1167–1176, DOI: **10.1211/jpp.58.9.0002**.

25 S. Gorantla, R. N. Saha and G. Singhvi, Spectrophotometric method to quantify tofacitinib in lyotropic liquid crystalline nanoparticles and skin layers: Application in ex

vivo dermal distribution studies, *Spectrochim. Acta, Part A*, 2021, **255**, 119719, DOI: **10.1016/j.saa.2021.119719**.

26 J. Bai, Y. Gao, L. Chen, Q. Yin, F. Lou, Z. Wang, *et al.*, Identification of a natural inhibitor of methionine adenosyltransferase 2A regulating one-carbon metabolism in keratinocytes, *EBioMedicine*, 2019, **39**, 575–590, DOI: **10.1016/j.ebiom.2018.12.036**.

27 S. Priya and G. Singhvi, Determination of 3-acetyl-11-keto-β-boswellic acid in analytical and biological samples using streamlined and robust RP-HPLC method, *Anal. Methods*, 2024, **16**(24), 3847–3858, DOI: **10.1039/d4ay00814f**.

28 R. Kashikar, A. K. Kotha, R. Shrestha, R. Channappanavar and M. B. Chougule, Design of experiments using box behnken design in the development, characterization, mathematical modeling, and evaluation of lung targeted nebulized antiviral camostat mesylate loaded pegylated nanosuspension product, *J. Drug Delivery Sci. Technol.*, 2024, **98**(February), 105810, DOI: **10.1016/j.jddst.2024.105810**.

29 A. Zafar, M. Yasir, D. S. Panda and L. Singh, Bergenin nano-lipid carrier to improve the oral delivery: Development, optimization, in vitro and in vivo evaluation, *J. Drug Delivery Sci. Technol.*, 2024, **96**(April), 105655, DOI: **10.1016/j.jddst.2024.105655**.

30 S. M. M. Moghddam, A. Ahad, M. Aqil, S. S. Imam and Y. Sultana, Optimization of nanostructured lipid carriers for topical delivery of nimesulide using Box–Behnken design approach, *Artif. Cells, Nanomed., Biotechnol.*, 2017, **45**(3), 617–624, DOI: **10.3109/21691401.2016.1167699**.

31 I. Chauhan, M. Yasir, M. Verma and A. P. Singh, Nanostructured lipid carriers: A groundbreaking approach for transdermal drug delivery, *Adv. Pharm. Bull.*, 2020, **10**(2), 150–165, DOI: **10.34172/apb.2020.021**.

32 M. Danaei, M. Dehghankhold, S. Ataei, F. Hasanzadeh Davarani, R. Javanmard, A. Dokhani, *et al.*, Impact of particle size and polydispersity index on the clinical applications of lipidic nanocarrier systems, *Pharmaceutics*, 2018, **10**(2), 1–17, DOI: **10.3390/pharmaceutics10020057**.

33 M. Dabbaghi, S. Namjoshi, B. Panchal, J. E. Grice, S. Prakash, M. S. Roberts, *et al.*, Viscoelastic and deformation characteristics of structurally different commercial topical systems, *Pharmaceutics*, 2021, **13**(9), 1–11, DOI: **10.3390/pharmaceutics13091351**.

34 V. Kakkar, I. P. Kaur, A. P. Kaur, K. Saini and K. K. Singh, Topical delivery of tetrahydrocurcumin lipid nanoparticles effectively inhibits skin inflammation: in vitro and in vivo study, *Drug Dev. Ind. Pharm.*, 2018, **44**(10), 1701–1712, DOI: **10.1080/03639045.2018.1492607**.

35 C. Olbrich, O. Kayser and R. H. Mu, Lipase degradation of Dynasan 114 and 116 solid lipid nanoparticles (SLN)—effect of surfactants, storage time and crystallinity, *Int. J. Pharm.*, 2002, **237**, 119–128, DOI: **10.1016/S0378-5173(02)00035-2**.

36 H. Saitoh, K. Takami, H. Ohnari, Y. Chiba, Y. Ikeuchi-Takahashi and Y. Obata, Effects and Mode of Action of Oleic Acid and Tween 80 on Skin Permeation of Disulfiram, *Chem. Pharm. Bull.*, 2023, **71**(4), 289–298, DOI: **10.1248/cpb.c22-00821**.